

<https://doi.org/10.51301/ejsu.2024.i5.03>

Electron microscopy of non-monocrystalline magnetron sputtered silicon thin films containing fibrous nanosilicon

K. Tolubaev¹, B. Zhautikov¹, N. Zobnin^{1*}, G. Dairbekova², S. Kabieva¹, Riad-Taha Al-Kasasbeh³

¹Karaganda Industrial University, Temirtau, Kazakhstan

²Satbayev University, Almaty, Kazakhstan

³University of Jordan, Amman, Jordan

*Corresponding author: zobninn@mail.ru

Abstract. The article examines the features of the microstructure of a new type of silicon film, based on a previously unstudied form of nanosilicon, obtained by magnetron sputtering. Microstructural analysis was carried out using a Jeol JSM-6490LA scanning electron microscope, a JEM2100 transmission electron microscope, and a Ntegra atomic force microscope (AFM) Thermo. Raman spectroscopic analysis of silicon films was carried out on a Horiba system Jobin – Yvon HR800UV (France). It has been established that the new form of nanosilicon under the studied conditions for obtaining silicon films is represented by fibers with a diameter of 10 to 150 nm. From a microstructural point of view, a silicon film, when a significant proportion of a new type of nanosilicon is formed in the film composition, acquires a porous cellular structure resulting from the interweaving of silicon nanofibers. The cells have an elongated oval shape with a width and length of about 1 and 3 μm , respectively. The obtained microphotographs are compared with similar data obtained when creating thin silicon films, which contain various polymorphic modifications of silicon in order to further classify the visual display of polymorphism and non-ideality of silicon nanostructures.

Keywords: *fibrous nanosilicon, electron microscopy, non-ideality, non-monocrystallinity, magnetron sputtering, amorphous silicon, crystalline silicon, film.*

1. Introduction

Traditional monocrystalline manufacturing methods are showing their limits, as evidenced by the slowing rate of transistor size reduction and the limited efficiency of crystalline solar cells [1-3]. To further improve the characteristics of functional elements, it is necessary to look for new approaches to creating nanostructures [4-6]. Modern advances in micro- and nanoelectronics demonstrate that the use of non-monocrystalline materials can lead to a breakthrough in the development of unique devices [7-8]. The absence of single crystallinity and the presence of various defects in the atomic lattice expand the properties of materials, providing them with new functions, such as flexibility and uniformity over large areas. In addition, non-monocrystalline silicon, including amorphous, micro- and nanocrystalline, opens up ways to reduce the cost of semiconductor device production [6]. The use of nanostructured silicon is in demand from the point of view of creating wide-gap materials, for example, silicon carbide, and expanding the spectrum closer to the ultraviolet range. The use of amorphous silicon increases the band gap and broadens the absorption spectrum. In addition, the influence of the energy levels of defect centers and dopant impurities can significantly improve the spectral dependences, both in the visible and in the infrared (IR) range, which in total will significantly increase the absorption band of photovoltaic structures [3, 12-14].

One of the most important characteristics of semiconductor structures is their optical spectral dependencies. The study of these dependencies makes it possible to identify ways to increase the mobility of charge carriers in thin-film transistors, charge-coupled devices and the efficiency of photoconverting elements [3, 4, 6]. This largely explains the widespread use of spectral methods for analyzing thin film structures in production conditions to assess the quality of the finished product. Such methods include Raman spectroscopy, diffractometry, IR spectroscopy and others. However, spectral methods often do not always make it possible to consider all the features of the obtained material. For example, for the technological properties of thin films, the types of geometric forms of polymorphic modifications of silicon, the relative position, the degree of localization of various forms, etc. are often important. There are many ways to produce thin films. Depending on the chosen method and deposition conditions, a number of features of the structure of the film and its constituent elements may differ in the presence of similar results of spectral analysis. In this regard, there is a need for direct visual study of thin films using various types of electron and atomic force microscopy, accumulation and classification of the resulting varieties of micro and nanostructures that arise during the formation of thin films. In this article, we summarize the experience that has previously been accumulated with respect to the microscopic analysis of non-monocrystalline silicon structures, and also present a new, previously unknown form of a silicon thin film component that can be identified as a type of nanosilicon.

One of the options for a visual description of nanosilicon is the statement that this polymorphic structure has a spherical shape with a diameter of 3-10 nm [12]. The same data are provided from other sources regarding the size of silicon nanospheres - 3.5-20 nm [13]. However, the authors did not provide the corresponding microphotographs. This statement is partially supported by the microphotograph shown in Figure 1, obtained by transmission microscopy, as well as the microphotograph shown in Figure 2, obtained by atomic force microscopy.

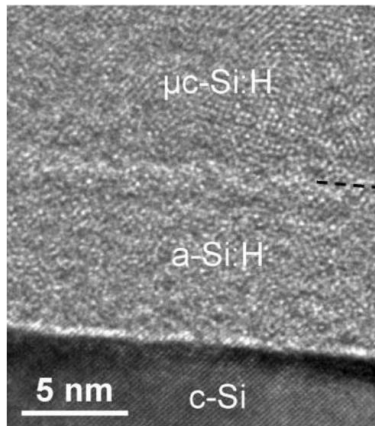


Figure 1. Micrograph of the atomic structure of single-crystalline, microcrystalline and amorphous silicon obtained using high-resolution transmission electron microscopy

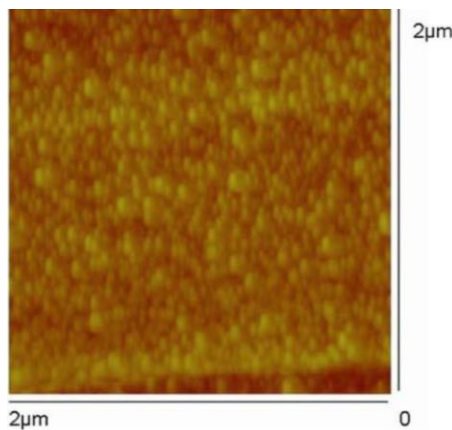


Figure 2. Micrograph of nanosilicon obtained using atomic force microscopy [15]

The film shown in Figure 1 was obtained by thermocatalytic chemical deposition (hot-wire chemical vapor deposition - HWCVD) when using a mixture of silane and hydrogen as precursors [14]. However, this image is difficult to accept as an image of nanoparticles. Judging by the scale here, we see some features of the atomic lattices of silicon, and not individual nanoparticles that have their own interface, limiting the collection of a certain set of silicon atoms. Even if we accept that we are observing nanoparticles, it should be noted that their sizes, judging from the image scale (about 0.1-0.3 nm), are much smaller than the sizes mentioned by the authors mentioned above [12, 13].

The film shown in Figure 2 was also obtained by the HWCVD method. The authors emphasize that this result was obtained as a result of strong dilution of silane with hydrogen (up to 95-98%). In this figure we also see spherical particles, but their size is much larger (about 100 nm) than the authors say [12, 13] and much larger than the authors say [14].

Another type of thin silicon film is amorphous films obtained in argon hydrogen plasma by magnetron sputtering. Films of amorphous and amorphous hydrogenated silicon (a-Si and a-Si:H) were obtained on magnetron installations of the type URM 3.279.014 and URM 3.279.026 (USSR) at a pressure in the working chamber of 10^{-2} - 10^{-3} Pa, voltage and target current – 500-650 V and 1.5-2 A, respectively [16]. The deposition rate was 0.1-0.4 $\mu\text{m}/\text{min}$, and the gas discharge current was 40 mA. The gas mixture in the magnetron chamber included argon and hydrogen. Films of amorphous and amorphous hydrogenated silicon were formed at different relative concentrations of hydrogen (0-60%), which were defined as the ratio of the partial pressure of hydrogen to the pressure of a mixture of argon and hydrogen. As substrates for the films under study, dielectrics (glass-ceramic substrates based on glass ceramics), semiconductors (p- and n-type crystalline silicon wafers, in order to create phase heterostructures - amorphous-crystalline material and conductors (based on brass, titanium, silver, beryllium bronze, aluminum foil) were used. Micrographs of this type of film are presented in Figure 3 [16].

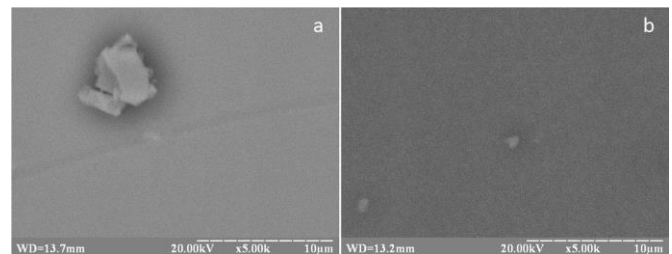


Figure 3. Defects on a-Si:H films: at a hydrogen content in plasma of 30% (a) and 50% (b) [16]

It is very difficult to compare previously discussed nanostructures (Figure 1-2) and amorphous structure (Figure 3). On the one hand, we can say that the amorphous structure is homogeneous and does not contain any signs of isolated micro or nano-sized particles with their own interface, with the exception of individual particles with characteristic signs of a crystalline nature 1-3 microns in size. However, it is quite possible that if we enlarge the images in Figure 3 to the level of Figure 2, we will see the same spherical particles with sizes of about 100 nm, which are not visible at the current magnification. In this regard, it is difficult to consider the visual difference between the nanocrystalline phase and the amorphous silicon phase as proven.

There are also microscopic studies of various polymorphic structures of a non-filmic nature. Powders not attached to a substrate are easier to study, because there is no problem with the ability to observe the features of the structures located inside the film. Nanocrystalline silicon powder was obtained by high-temperature plasma-chemical synthesis. Water was used as a coolant and argon as a buffer gas. The starting material was silicon, crushed into microcrystalline powder with particle sizes of tens of micrometers [17, 18].

Figure 4 shows micrographs of the surface structure of powder nanosilicon (pwSi) obtained in this way. These photographs allow you to evaluate the shape and size of microparticles of the powder material. As can be seen from the figure, the powder is characterized by microcrystals and tubular structures [1, 7, 18].

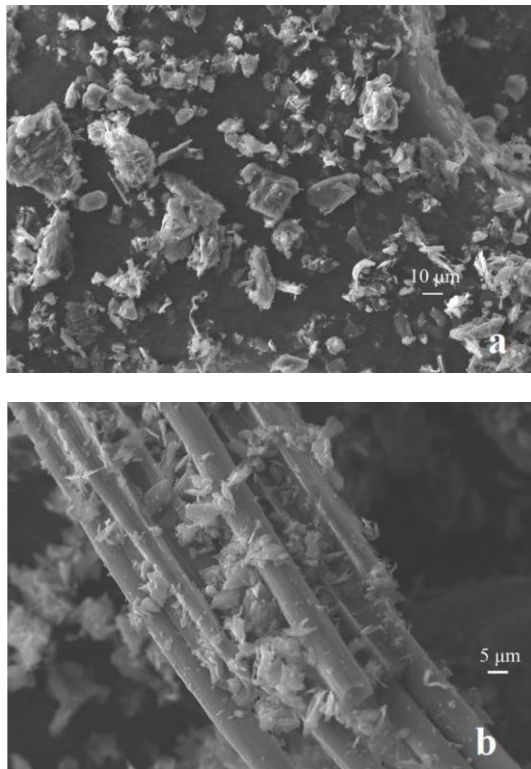


Figure 4. Microparticles (a) and microtubes (b) of powdered silicon at magnification using an electron microscope [17, 18, 19]

Figure 4 shows that powdered silicon has individual microparticles, and their complex branched surface relief is visible. Both individual microtubes and their clusters are present. Microparticles are also observed near the surface of tubular structures. However, Figure 4 does not allow nanocrystallites to be seen. In this regard, high-magnification electron microscopy was also used, as shown in Figure 5 [19]. The spherical particles shown in Figures 1 and 2 are also not visible in Figure 5. The authors note that the powder consists of silicon microparticles with a large number of nanocrystallites on their surface. Figure 5 (c) shows that the silicon microparticle has a porous, loose spongy structure; however, it is quite difficult to talk about the presence of nanocrystallites at this magnification. And only after an even greater magnification of the image of the same particle, the presence of nanocrystallites becomes obvious. With the magnification shown in Figure 6, we can confidently say that the material is represented by spherical nanocrystallites with a diameter of about 100-150 nm, i.e. the result of microscopy of silicon powder coincided with the result of microscopy of silicon film, presented here in Figure 2. According to the authors, the electron diffraction pattern presented in Figure 6 (b) is a set of concentric circles (rings), which proves the micro-nanocrystalline structure of the substance.

In general, it should be noted that despite the key importance of silicon films in modern science and production in the fields of electronics, photovoltaics, electrical energy storage, etc., information about the features of the micro and nanostructure of these films is very contradictory. Theoretical studies on this issue often do not agree with practical data obtained by various microscopy methods. Meanwhile, the lack of classified data on this matter greatly complicates the targeted optimization of the technical properties of silicon films. This article is devoted to this problem.

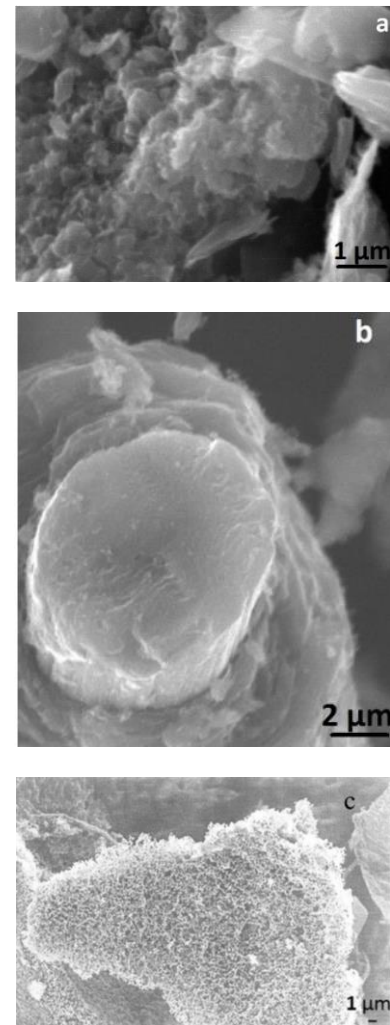


Figure 5. The surfaces of particles shown in Figure 4 at a higher magnification: microparticles (a), microtubes (b), microparticles with nanocrystallites on the surface (c) [19]

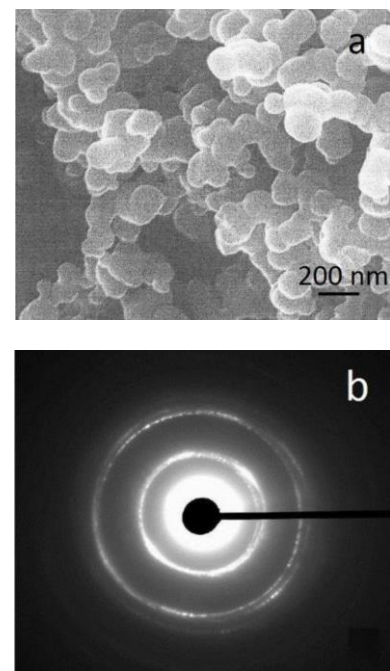


Figure 6. Nanocrystallites on the surface of powdered silicon particles, shown in Figure 5 (c) at high magnification (a) and its electron diffraction pattern (b) [19]

2. Materials and methods

For microscopic examination, several types of silicon nanofilms were synthesized under various technological conditions of magnetron sputtering using the Caroline D12C system. Silicon crystals grown by the Czochralski method using commercial high-purity silicon of SoG-Si grade 6-7N were used as targets for magnetron sputtering. The substrate was copper foil 0.5 mm thick. The thickness of the silicon film was 300-400 nm.

Microstructural analysis was carried out using three types of equipment. By comparing the obtained parallel micrographs, we selected those that most qualitatively demonstrated the features of the micro and nanostructure of silicon films. Microscopy equipment used:

1. Electronic transmission microscope JEM 2100. Magnification of the microscope from 50 to 1 500 000 times allows you to fully study the atomic crystal structure of the material, including the morphology and characteristics of the crystal structure, characteristics of the type and distribution of various defects in the crystal structure (grain boundaries, stacking faults, dislocations, various combinations of point defects), as well as carry out a chemical analysis of particles and various inclusions released in alloys (including gas bubbles, voids), and study the domain structure;

2. Scanning electron microscope JEOL JSM-6490LA, used to determine chemical elements, microanalysis to determine the elemental composition of the sample, as well as to determine the thickness of the resulting silicon films;

3. Atomic force microscope (AFM) Ntegra Therna. AFM is a modern method for studying surfaces and surface properties.

The polymorphism of silicon films was clarified using Raman spectroscopy. Raman spectroscopic analysis was carried out on a Horiba brand system Jobin-Yvon HR800UV (France). An argon-cadmium laser with a wavelength of 315 nm was used as the excitation source. The laser power on the sample was ~25 mW for Ar / Cd. The holographic diffraction grating had 2200 lines/mm for a 315 nm laser and was focused onto a CCD detector. The lens was Olympus 412 UV for Ar / Cd. The measurements were carried out in the range from 0 to 3200 cm^{-1} . No filter was used to reduce the radiation entering the detector from the samples.

3. Results and discussion

All thin silicon films that were obtained during the study under various conditions of magnetron sputtering can be divided into two main types. For each sample, several parallel microscopic observations were carried out at several different points along the entire surface of the film. This test showed the uniformity of the morphology of the entire surface of each type of film, which indicates the advantage of magnetron sputtering technology over the CVD method in terms of ensuring film uniformity. According to the available literature data, films produced by CVD are extremely heterogeneous in terms of polymorphism [12]. Figure 7 shows micrographs of the first type of silicon film.

A preliminary examination of the microphotographs shows that the structure of the first type of silicon film is visually represented by crystalline and amorphous silicon in approximately comparable proportions with a predominance of the amorphous component.

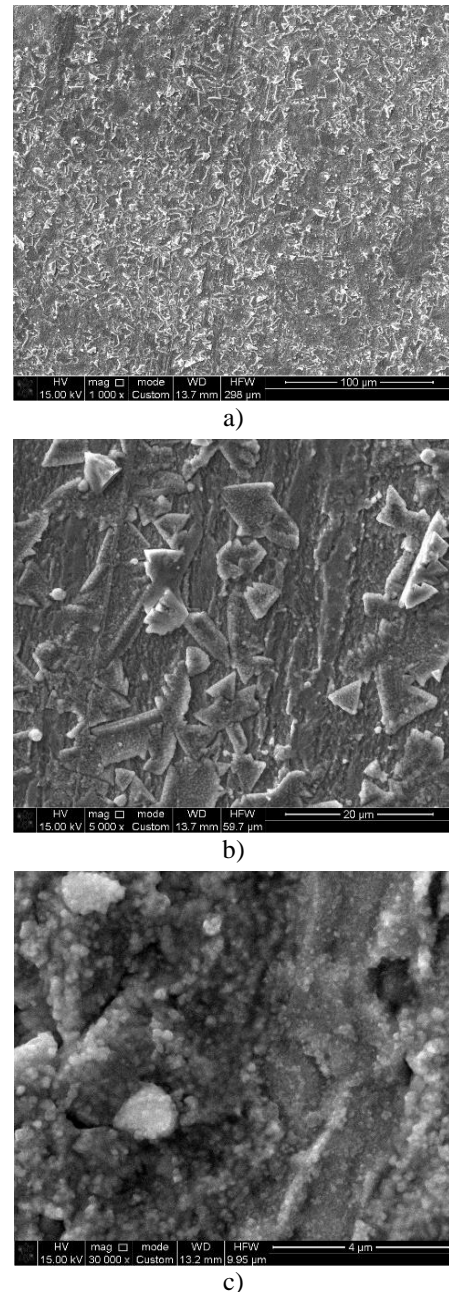


Figure 7. Micrograph of the surface of a silicon film of the first type (a combination of amorphous and crystalline silicon) at magnification: (a) $\times 1000$; (b) $\times 5000$; (c) $\times 30000$

Figure 8 shows photographs of the second type of silicon film at different magnifications. Comparison of photographs in Figures 7 and 8 shows a fundamental change in the structure of the silicon film. Visually, one can see the appearance of a nanosilicon structure that has not previously been found in the literature. Unlike the spherical particles that we observed previously, the new nanosilicon structure has the form of intertwined fibers with a diameter of 10 to 150 nm. One could assume that this form has common features with the already known form of microtubes, presented in Figure 4. However, unlike new silicon nanofibers, microtubes have a rigid shape, which does not provide the possibility of interlacing, and their diameter is much larger - from 5 to 10 μm . From a microstructural point of view, the new type of silicon film acquires a porous cellular structure resulting from the interweaving of silicon nanofibers. The cells have an elongated oval shape with a width and length of about 1 and 3 μm , respectively.

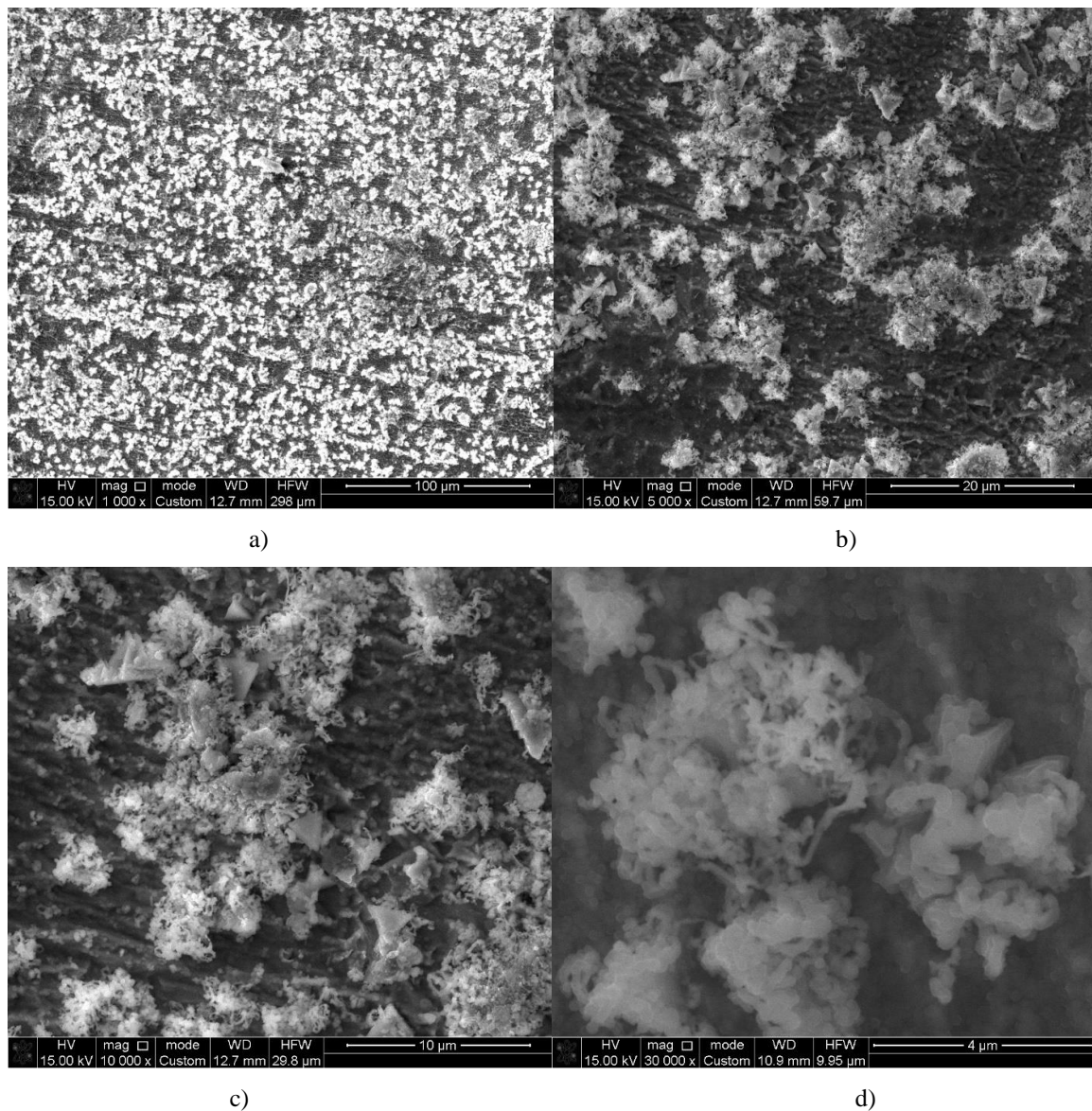


Figure 8. Micrograph of the surface of a second type of silicon film (a new type of fibrous nanosilicon) at magnification: (a) $\times 1000$; (b) $\times 5000$; (c) $\times 10000$; (d) $\times 30000$

Comparing the conditions under which silicon films were obtained, it can be tentatively assumed that the emergence of a new type of silicon nanofilm is associated with an increase in pressure during magnetron sputtering, which leads to the appearance of a nanosilicon phase against the background of a reduction in the amorphous and, to a greater extent, crystalline phases. However, with a simultaneous increase in the specific power at the target and the pressure in the working chamber, the proportions of the amorphous and nanocrystalline phases of silicon decrease due to an increase in the proportion of the crystalline phase.

In addition, a significant increase in the fraction of nanosilicon from 45.6 to 64.0% may be associated with an increase in the voltage pulse frequency applied to the target. Arbitrary variation of the magnetron sputtering parameters indicated above leads to ambiguous changes in the ratio of polymorphic forms of silicon in the film. From this, we can conclude that there are some optimal values of these parameters and they can be detected basing on mathematical modeling of multifactorial dependence. This requires additional experiments, which will be carried out in the future.

4. Conclusions

In the process of microscopic examination of magnetron sputtering products - silicon films, a previously unknown polymorphic modification - fibrous nanosilicon was identified, and the result of obtaining crystalline silicon was reproduced. The new silicon film obtained under experimental conditions acquires a porous cellular structure resulting from the interweaving of silicon nanofibers with a diameter of 10 to 150 nm. The cells have an elongated oval shape with a width and length of about 1 and 3 μm , respectively. This form is fundamentally different from the previously described form of nanosilicon as spherical particles with a diameter of about 100 nm. It has been established that the greatest influence on increasing the proportion of new nanosilicon in the film composition is exerted by an increase in the pressure in the working chamber and the frequency of voltage pulses on the target.

An increase in the specific power at the target leads to a reduction in the proportion of the amorphous phase and an increase in the crystalline phase, but this indicator does not

affect the increase in the proportion of nanocrystalline silicon. Increasing the pressure in the working chamber and the voltage frequency helps to increase the proportion of nanosilicon. However, there is probably a limit to these parameters, beyond which a further increase in their values reduces the share of nanosilicon.

Additional experiments are needed to identify more accurate optimal values of magnetron sputtering parameters and to test the resulting silicon films as anodes of lithium-ion batteries. Parallel microscopic measurements showed the uniformity of the polymorphic composition of both types of films, which confirms the advantages of magnetron sputtering technology over the CVD method.

References

- [1] Dai, X. (2017). Improving convergence and simulation time of quantum hydrodynamic simulation: Application to extraction of best 10-nm FinFET parameter values. *IEEE Transactions on Very Large Scale Integration (VLSI) Systems*, 25(1), 319-329. <https://doi.org/10.1109/TVLSI.2016.2564300>
- [2] Goli, M.H., González-Vélez, H. (2017). Autonomic coordination of skeleton-based applications over CPU/GPU multi-core architectures. *International Journal of Parallel Programming*, 45 (2), 203–224. <https://doi.org/10.1007/s10766-016-0419-4>
- [3] Green, M.A., Hishikawa, Y., Warta, W. (2017) Solar cell efficiency tables (version 50). *Progress in Photovoltaics*, 25(7), 668–676. <https://doi.org/10.1002/pip.2909>
- [4] Chebotarev, S.N., Kalinchuk, V.V. & Lunin, L.S. (2016). Semiconductor nanoheterostructures with an intermediate subband. *M.: Physics and Mathematics Literature*
- [5] Chen, Y., Zhang, H. & Zhu Y. (2002). A new method of fullerene production: pyrolysis of acetylene in high-frequency thermal plasma. *Materials Science and Engineering*, 95 (1), 29–32. [https://doi.org/10.1016/s0921-5107\(02\)00130-7](https://doi.org/10.1016/s0921-5107(02)00130-7)
- [6] Afanasyev, V.P., Terukov, E.I. & Sherchenkov, A.A. (2011). Thin-film solar cells based on silicon. *St. Petersburg: Publishing house of St. Petersburg Electrotechnical University «LETI»*
- [7] Sattler, K.D. (2016). Carbon Nanomaterials Sourcebook: Graphene, Fullerenes, Nanotubes, and Nanodiamonds (Volume 1). *CRC Press*
- [8] Fabry, F., Gruenberger, T.M. & Aguilar, J.G. (2005). Continuous mass production of fullerenes and fullerene nanoparticles by 3-phase AC plasma processing. *NSTI Nanotech Technical Proceedings*, 3, 201–204
- [9] Behera, S.N., Gayen, S., Ravi Prasad G.V. & Bose, S. (2007). Electronic properties of ordered and disordered linear clusters of atoms and molecules. *Physica*, 390, 124–133. <https://doi.org/10.1016/j.physb.2006.08.018>
- [10] Zhigunov, D.M., Ilyin, A.S. & Forsh, P.A. (2017). Luminescence of solar cells with a - Si : H / c - Si heterojunction. *Letters to the Journal of Theoretical Physics*, 43(10), 95–101. <https://doi.org/10.1134/S1063785017050261>
- [11] Thevaril, J., O'Leary, S.K. (2010). Defect absorption and optical transitions in hydrogenated amorphous silicon. *Solid State Commun*, (150), 1851–1855. <https://doi.org/10.1016/j.ssc.2010.06.034>
- [12] Gaisler, S.V., Semenova, O.I., Sharafutdinov, R.G. & Kolesov, B.A. (2004). Analysis of Raman spectra of amorphous- nanocrystalline silicon films. *Solid State Physics*, 46(8), 1484-1488. <https://doi.org/10.1134/1.1788789>
- [13] Kamei, T., Stradins, P. & Matsuda, A. (1999). Effects of embedded crystallites in amorphous silicon on light-induced defect creation. *Applied Physics Letters*, 74(12), 1707-1709. <https://doi.org/10.1063/1.123662>
- [14] Olibet, S., Vallat-Sauvain, E. & Fesquet, L. (2010). Properties of interfaces in amorphous/crystalline silicon heterojunctions. *Phys. Status Solidi A*, 207(3), 651–656. <https://doi.org/10.1002/pssa.200982845>
- [15] Esmaili Rad, M.R., Sazonov, A. & Kazanskii, A.G. (2007). Optical properties of nanocrystalline silicon deposited by PECVD. *Journal of Materials Science: Materials in Electronics*, 18, P. 405–409. <https://doi.org/10.1007/s10854-007-9230-8>
- [16] Mazinov, A., Shevchenko, A. & Bahov, V. (2014). Quantum interactions of optical radiation with the defect centers in the tails of the forbidden band of amorphous materials. *Optica Applicata*, 44(2), 327–335. <https://doi.org/10.5277/oa140213>
- [17] Mazinov, A.S., Shevchenko, A.I. & Voskresensky, V.M. (2014). Nanostructured semiconductors obtained by powder method. *Scientific notes of the Tauride National University named after V.I. Vernadsky, Series Physical and Mathematical Sciences*, 27 (66), 107–114
- [18] Mazinov, A.S., Shevchenko, A.I., Voskresensky, V.M. & Kuropatkin A.V. (2014). Nanostructured semiconductors based on powder technology. *24th International Crimean Conference «Microwave Engineering and Telecommunication Technologies (CriMiKo'2014)»*, Sevastopol
- [19] Mazinov, A.S., Shevchenko, A.I., Voskresensky V.M. (2015). Silicon-carbon structures for modern micro- and nanoelectronics. *25th International Crimean Conference «Microwave Engineering and Telecommunication Technologies (CriMiKo'2015)»*, Sevastopol

Талшықты нано кремний бар магнетронды шашыратылған монокристалды емес кремнийлі жұқа қабықшалардың электронды микроскопиясы

Қ. Толубаев¹, Б. Жаутиков¹, Н. Зобнин^{1*}, Г. Даирбекова², С. Кабиева¹, Риад-Таха Ал-Касабх³

¹Қарағанды индустриялық университеті, Теміртау, Қазақстан

²Satbayev University, Алматы, Қазақстан

³Иордания университеті, Амман, Иордания

*Корреспонденция үшін автор: zobninn@mail.ru

Андатпа. Мақалада магнетронды бүрку арқылы алынған нано кремнийдің бұрын зерттелмеген түріне негізделген кремний пленкасының жаңа түрінің микроқұрылымының ерекшеліктері қарастырылады. Микроқұрылымдық талдау JEOL JSM-6490LA растрлық электронды микроскопында, JEM2100 электронды трансмиссиялық микроскопында және Ntegra Thermo атомдық күштік микроскопында (AFM) жүргізілді. Кремний пленкаларының Раман спектроскопиялық талдауы Horiba system Jobin – Yvon HR800UV (Франция) маркалы жүйесінде жүргізілді. Кремний пленкаларын алудың зерттелген жағдайында нано кремнийдің жаңа түрі диаметрі 10-нан 150 нм-ге дейінгі талшықтармен

ұсынылатыны анықталды. Микроқұрылымдық тұрғыдан алғанда, кремний пленкасы нано кремний талшықтарының бір-бірімен араласуы нәтижесінде пайда болатын кеукті жасушалық құрылымға ие болады. Жасушалардың ені мен ұзындығы сәйкесінше 1 және 3 мкм болатын ұзартылған сопақша пішіні бар. Алынған микрографтар полиморфизмнің визуалды картасын әрі қарай жіктеу және кремнийдің нано құрылымдарының идеалдығын емес, құрамында кремнийдің әртүрлі полиморфты модификациялары бар жұқа кремний пленкаларын жасау кезінде алынған ұқсас деректермен салыстырылады. Зерттеу барысында алынған кеукті құрылымы бар нано өлшемді кремний анодтары LIB зарядтау процесінде литизацияға тезірек ұшырайды және цикл арқылы аз ыдырайтыны анықталды.

Негізгі сөздер: талшықты наносиликон, электронды микроскопия, идеалдылық емес, монокристалдылық емес, магнетрондық шашырау, аморфты кремний, кристалды кремний, қабықша.

Электронная микроскопия не монокристаллических тонких кремниевых плёнок магнетронного напыления, содержащих волокнистый нанокремний

К. Толубаев¹, Б. Жаутиков¹, Н. Зобнин^{1*}, Г. Даирбекова², С. Кабиева¹, Риад-Таха Ал-Касахбех³

¹Карагандинский индустриальный университет, Алматы, Казахстан

²Satbayev University, Алматы, Казахстан

³Университет Иордании, Амман, Иордания

*Автор для корреспонденции: zobninn@mail.ru

Аннотация. В статье рассмотрены особенности микроструктуры нового типа кремниевой плёнки, на базе ранее не изученной формы нано кремния, полученных методом магнетронного напыления. Микроструктурный анализ проводили на растровом электронном микроскопе Jeol JSM-6490LA, электронном просвечивающем микроскопе JEM2100 и атомно-силовом микроскопе (АСМ) Ntegra Therna. Рамановский спектроскопический анализ кремниевых плёнок проводился на системе марки Horiba Jobin–Yvon HR800UV (Франция). Установлено, что новая форма нано кремния в изученных условиях получения кремниевых плёнок представлена волокнами диаметром от 10 до 150 нм. С микроструктурной точки зрения плёнка кремния при формировании значительной доли нано кремния нового типа в составе плёнки приобретает пористую ячеистую структуру, возникающую в результате переплетения нано волокон кремния. Ячейки имеют вытянутую овальную форму шириной и длиной около 1 и 3 мкм соответственно. Полученные микрофотографии сопоставлены с аналогичными данными, полученными при создании тонких кремниевых плёнок, которые имеют в своём составе различные полиморфные модификации кремния с целью дальнейшей классификации визуального отображения полиморфизма и не идеальности нано структур кремния. Предположительно, выявленные в ходе исследования нано размерные кремниевые аноды с пористой структурой будут быстрее подвергаться литированию в процессе зарядки LIB и меньше будут разрушаться в результате циклирования.

Ключевые слова: волокнистый нано кремний, электронная микроскопия, не идеальность, не монокристалличность, магнетронное напыление, аморфный кремний, кристаллический кремний, плёнка.

Received: 05 July 2024

Accepted: 15 October 2024

Available online: 31 October 2024